〈論文〉 4-5-1

펄스폭 변조 직렬공진 컨버터의 제어연구

崔 鉉 七

Control Methods of the Pulse-Width Modulated Series Resonant Converter(PWM-SRC)

Hyun-Chil Choi

요 약

본 연구에서는 선형화 소신호 모델을 이용하여 불연속 모드 펄스폭 공진회로의 다양한 제어방법에 대하여 조사하였다. 각 제어방식에 따른 시스템의 안정도와 동적 특성을 분석하기 위하여 정규화 출력 전류와 전압을 사용한 근궤적을 나타내었다. 또한, 최적의 궤적 특성을 가지는 제어기를 새로이 제안하였으며, 이러한 제어의 우수한 특성을 다른 형태의 제어방식과 비교함으로써 입증하였다.

ABSTRACT

In this paper, several control methods for the discontinuous mode PWM-SRC are investigated with the linearized small signal model. In order to analyze the stability and dynamic characteristics of the controlled system, the root locus as a function of the normalized output current(NOC) for a given normalized output voltage(NOV) is employed. Furthermore, in this paper, the "Optimal trajectory control of PWM-SRC" is newly proposed and its good dynamic performances are evaluated with other four control laws.

Key Words : Pulse-Width modulated SRC, Optimal-trajectory control

1. Introduction

In view of the basic control concept, the conventional series resonant converters(SRC) can be generally classified into two categories such as a frequency domain control and a phase domain control. In case of a frequency domain control, the ratio of the switching frequency to the resonant frequency is controlled to obtain a desirable output. In case of a phase domain control, the pulse width modulation(PWM) method has been applied to the SRC and the output is controlled by shifting the phase or adjusting the turn on time of the gating signals. Since, in a frequency domain controlled SRC, the output voltage largely depends upon the load and line conditions as well as the switching frequency, the filter design is difficult[1-3]. In view of this point, a pulse width modulation series resonant converter(PWM-SRC) is more advantageous than a frequency domain control scheme. Due to the fixed switching frequency, the values of the filter and magnetic components can be easily optimized[4-6]. Furthermore, employing the discontinuous mode operation, the lower switching stress can be also obtained.

To investigate the stability and dynamic

performances of the PWM-SRC, a linearized small signal modelling method is recently introduced[6]. However, only the transistor conduction angle control method is examined in this research. Therefore, in this paper, the effect of different controllers on the closed-loop dynamics are examined to better control the PWM-SRC. Especially, the optimal-trajectory control scheme with the superior dynamic performance is newly proposed. In order to analyze the stability and dynamic performances of the controlled system, the root locus as a function of the normalized output current(NOC) for a given normalized output voltage(NOV) is employed. It is intended to examine how the load variation for a given NOV affects the stability and dynamic characteristics of the controlled system. From the root locus results, the excellent dynamic performance of the proposed optimal-trajectory control can be easily expected. Also, these are verified through the simulation results.

2. Review of small signal model for the PWM-SRC

A description of the operation and the small signal modelling for a PWM-SRC with discontinuous mode is briefly discussed in this section. For detailed explanations, refer to[6].

Fig. 1 shows a circuit diagram of the multi-loop controlled PWM-SRC with discontinuous mode. In this circuit, the inner feedback loop is for the pulse-by-pulse control of an inductor current or capacitor voltage and the outer loop is used to regulate the output voltage. The discrete state variables of the PWM-SRC are defined in Fig. 2 and the equivalent circuit is shown in Fig. 3. In Fig. 2, taking the inductor current and the capacitor voltage at the switching instant (t_k, t_{k+1}) as the state variables, these become

$$x_1(t_k) = -i_L(t_k), \quad x_2(t_k) = -v_c(t_k), \text{ and } x_3(t_k) = v_o(t_k) \text{ at } t = t_k \tag{1}$$

$$x_1(t_{k+1}) = i_L(t_{k+1}), \quad x_2(t_{k+1}) = v_c(t_{k+1}) \text{ at } t = t_{k+1}. \tag{2}$$

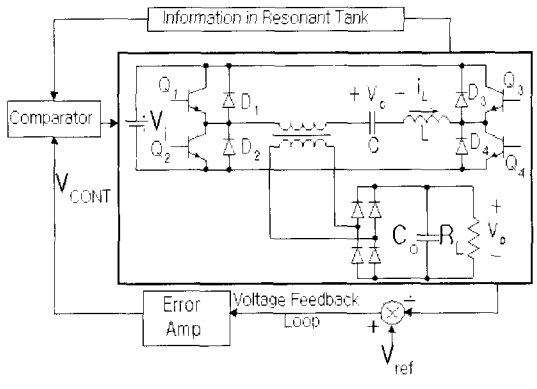

Fig. 1 Block diagram of multi-loop controlled PWM-SRC

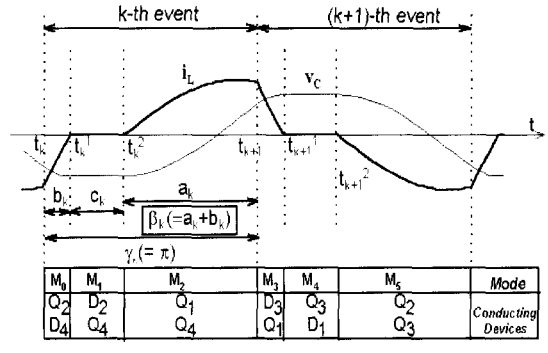

Fig. 2 Waveforms of PWM-SRC under transistor-conduction angle control

	V_E	i_L Polarity
M_0	V_o	-
M_1	$-V_o$	+
M_2	$V_i - V_o$	+
M_3	$-V_o$	+
M_4	V_o	-
M_5	$-V_i - V_o$	-

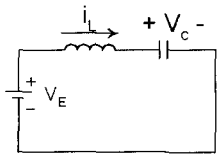

Fig. 3 Equivalent input voltage and circuit for each topological mode

Then, the nonlinear discrete time domain representation of the resonant tank for the k-th event can be obtained as follows :

$$x_1(t_{k+1}) = x_1(t_k) \cdot \sin(a_k) \cdot \sin(b_k) + (x_2(t_k)/Z) \cdot \sin(a_k) \cdot \cos(b_k) + (x_3(t_k)/Z) \cdot \sin(a_k) \cdot (-2 + \cos(b_k)) + (v_i/Z) \cdot \sin(a_k) \quad (3)$$

$$x_2(t_{k+1}) = -x_1(t_k) \cdot Z \cdot \cos(a_k) \cdot \sin(b_k) - x_2(t_k) \cdot \cos(a_k) \cdot \cos(b_k) + x_3(t_k)((2 - \cos(b_k)) \cdot \cos(a_k) \cdot -1) + v_i(1 - \cos(a_k)) \quad (4)$$

$$x_3(t_{k+1}) = -x_3(t_k) + (\frac{C}{C_o}) \cdot \{Z \cdot (2 - \cos(a_k)) \cdot \sin(b_k) \cdot x_1(t_k) - (1 + (\cos(b_k) \cdot (\cos(a_k) - 2)) \cdot x_2(t_k) + [1 + (\cos(a_k) - 2) \cdot (2 - \cos(b_k) - \frac{Z}{R_L} \cdot \gamma_k] \cdot x_3(t_k) + v_i \cdot (1 - \cos(a_k))\} \quad (5)$$

where

$$Z = \sqrt{\frac{L}{C}}, \quad \omega = \frac{1}{\sqrt{LC}}, \quad a_k = \omega(t_{k+1} - t_k^2),$$

$$b_k = \tan^{-1}(\frac{Z \cdot x_1(t_k)}{x_2(t_k) + x_3(t_k)}),$$

$$\gamma_k = \omega(t_{k+1} - t_k) = a_k + b_k + c_k = \pi .$$

From the steady state condition of $x(t_k) = x(t_{k+1}) = x = constant$, the steady state solutions are

$$x_1 = \frac{v_i \cdot \sin(a) \cdot \sin(b)}{Z \cdot \sin(\beta)} \quad (6)$$

$$x_2 = \frac{v_i \cdot (2\sin(a) \cdot \cos(b) - \sin(\beta) - \sin(a) + \sin(b))}{Z \cdot \sin(\beta)} \quad (7)$$

$$x_3 = \frac{v_i \cdot (\sin(\beta) + \sin(a) - \sin(b))}{2\sin(\beta)} \quad (8)$$

where

$$b = \sin^{-1} \cdot (\frac{v_i \cdot \sin(a)}{\sqrt{(-v_i + 2x_3)^2 + 2(-v_i + 2x_3) \cdot \cos(a) \cdot v_i + v_i^2}}) - \tan^{-1}(\frac{(-v_i + 2x_3) \cdot \sin(a)}{(-v_i + 2x_3) \cdot \cos(a) \cdot v_i + v_i})$$

$$\beta = a + b .$$

Since the discrete time domain equations (3), (4) and (5) have the nonlinearity, it is difficult to derive the general input-output transfer function. Therefore, considering the small perturbations about the operating values, the state equations can be linearized.

Employing the transistor-conduction angle control, the linearized state equation for the discontinuous PWM-SRC can be obtained as follows[6].

$$\delta X(t_{k+1}) = G \cdot \delta X(t_k) + H \cdot \delta U_k \quad (9)$$

where

$$\delta X(t_k) = [\delta x_1(t_k) \quad \delta x_2(t_k) \quad \delta x_3(t_k)]^T$$

$$\delta X(t_{k+1}) = [\delta x_1(t_{k+1}) \quad \delta x_2(t_{k+1}) \quad \delta x_3(t_{k+1})]^T$$

$$\delta U_k = [\delta a_k \quad \delta v_i(t_k)]^T$$

$$g_{11} = \sin(a) \cdot \sin(b), \quad g_{12} = \frac{\sin(a) \cdot \cos(b)}{Z}$$

$$g_{13} = \frac{\sin(a) \cdot (\cos(b) - 2)}{Z}, \quad h_{11} = \frac{(v_i - x_2 - x_3)}{Z}$$

$$h_{12} = \frac{\sin(a)}{Z}, \quad g_{21} = -Z \cdot \cos(a) \cdot \sin(b)$$

$$g_{22} = -\cos(a) \cdot \cos(b)$$

$$g_{23} = (2 - \cos(b)) \cdot \cos(a) - 1$$

$$h_{21} = Z \cdot x_1, \quad h_{22} = 1 - \cos(a)$$

$$g_{31} = NC \cdot Z \, [(2 - \cos(a)) \cdot \sin(b) - PP1 \cdot \frac{x_3}{R_L}]$$

$$g_{32} = NC \, [-1 + \cos(b) \cdot (2 - \cos(a)) - PP2 \cdot Z \cdot \frac{x_3}{R_L}]$$

$$g_{33} = 1 + NC \, [1 + (\cos(a) - 2) \cdot (2 - \cos(b)) - \frac{Z}{R_L} \cdot \gamma_k] - PP3 \cdot NC \cdot Z \cdot \frac{x_3}{R_L}$$

$$h_{31} = NC \cdot Z \, [x_1 - \frac{x_3}{R_L}], \quad h_{32} = NC \cdot (1 - \cos(a))$$

$$PP1 = \frac{(x_2 + x_3) \cdot Z}{(Z \cdot x_1)^2 + (x_2 + x_3)^2}$$

$$PP2 = \frac{-Z \cdot x_1}{(Z \cdot x_1)^2 + (x_2 + x_3)^2}, \quad PP3 = PP2$$

$$PPV = 0, \quad NC \frac{C}{C_o} .$$

3. Control Methods of the PWM-SRC

3.1 Liberalization of Control Laws

As can be seen in Fig. 2, the control action is applied at $t=t_{k+1}$ and the control law can be expressed as a function of the state variables. Some control methods which have been applied to the resonant converters are employed and the optimal trajectory control is proposed for the PWM-SRC control. A brief description of these control methods are explained in the following.

3.1.1 ASDTIC Control

The control law is

$$\int_k^{k+1}(|i_L|-V_{cont})dt=0 \tag{10}$$

where V_{cont} is the control signal of the controlled PWM-SRC determined by the control law. Using the state variables, equation (10) becomes

$$\begin{aligned}&(2-\cos(a_k))\cdot\sin(b_k)\cdot x_1(t_k)-[1+\cos(b_k)\\&\cdot(\cos(a_k)-2)]\cdot x_2(t_k)/Z+[1+(\cos(a_k)-2)\\&(2-\cos(b_k))]\cdot x_3(t_k)/Z+v_i\cdot(1-\cos(a_k))/Z\\&-\gamma_k\cdot V_{cont}=0\ .\end{aligned} \tag{11}$$

Under the steady-state, the following condition is satisfied as

$$V_{cont}|_{op}=x_3/R_L. \tag{12}$$

Linearizing (11) about the operating point gives

$$\begin{aligned}\gamma_k\cdot\delta V_{cont}=&[(2-\cos(a_k))\cdot\sin(b_k)-x_3\\&\cdot PP1/R_L]\cdot\delta x_1(t_k)-\{[1+\cos(b_k)\\&\cdot(\cos(a_k)-2)]/Z+x_3\cdot PP2/R_L\}\cdot\delta x_2(t_k)\\&+\{[1+(\cos(a_k)-2)\cdot(2-\cos(b_k))]/Z\\&-x_3\cdot PP3/R_L\}\cdot\delta x_3(t_k)+[(1-\cos(a_k))/Z]\\&\cdot\delta v_i(t_k)+(x_1-x_3/R_L)\cdot\delta a_k\ .\end{aligned} \tag{13}$$

3.1.2 Inductor-Current Control

The control law is

$$V_{cont}=x_1(t_{k+1}) \tag{14}$$

and linearizing (14) gives

$$\delta V_{cont}=\delta x_1(t_{k+1})\ . \tag{15}$$

3.1.3 Capacitor-Voltage Control

The control law of the capacitor-voltage control is

$$V_{cont}=x_2(t_{k+1}) \tag{16}$$

and linearizing (16) gives

$$\delta V_{cont}=\delta x_2(t_{k+1})\ . \tag{17}$$

3.1.4 Optimal-Trajectory Control of PWM-SRC

For the PWM-SRC operating in the discontinuous conduction mode, the control law of the optimal trajectory control is newly developed as

$$V_{cont}=\sqrt{(Z\cdot x_1(t_{k+1}))^2+(x_3(t_{k+1})+x_2(t_{k+1}))^2} \tag{18}$$

This proposed control law is continuously monitoring the energy levels of the resonant tank and has the time-optimal dynamics. Fig. 4 shows the trajectory response on the state-space for a step change in a control input from V_{cont1} to V_{cont2} .

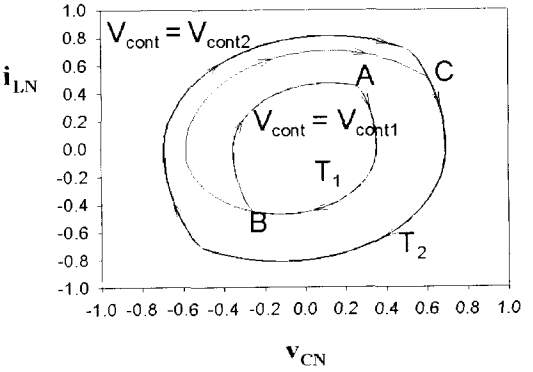

Fig. 4 Response of optimal-trajectory control for step control change where vCN, iLN are he normalized state variables with Vi and i/Zo as the normalized factors, respectively

With the control input V_{cont1}, the system is on the trajectory T_1. the control input is changed into V_{cont2} when the state travels between point A and B on T_1. Since V_{cont} is not equal to the new control input V_{cont2} at the point B, the switching action is not occurred and the conduction is continued until the state trajectory reaches point C where V_{cont} equals V_{cont2} . At point C, the switching action is occurred and the system is now on the trajectory T_2 . Therefore, utilizing this control law, the states of the system can reach optimally the new steady-state in timewise. Through the linearization of (18) about the steady-state, the following is obtained as

$$\delta V_{cont}=\frac{Z^2\cdot x_1}{\sqrt{(Z\cdot x_1)^2+(x_3+x_2)^2}}\cdot\delta x_1(t_{k+1})+\frac{(x_3+x_2)}{\sqrt{(Z\cdot x_1)^2+(x_3+x_2)^2}}\cdot\delta x_2(t_{k+1}). \quad (19)$$

For the four control law described above, the following generalized form can be derived using the elements of (9) as

$$\delta a_k=-K_1\cdot\delta x_1(t_k)-K_2\cdot\delta x_2(t_k)-K_3\cdot\delta x_3(t_k)+K_4\cdot\delta V_{cont}-K_5\cdot\delta v_i(t_k)\ . \quad (20)$$

and coefficients of (20) for each control law are presented in Table 1.

3.2 Linearization of the Controlled PWM-SRC

Combining the linearized PWM-SRC and the control law, the linearized small signal model can be obtained for the controlled PWM-SRC. Substituting (20) into (9) gives

$$\delta X(t_{k+1})=G_c\cdot\delta X(t_k)+H_c\cdot\delta U_{ck} \quad (21)$$

where

$$\delta U_{ck}=[\,\delta V_{cont}\quad \delta v_i(t_k)\,]^T$$

$$G_c=\begin{bmatrix} g_{11}-h_{11}K_1 & g_{12}-h_{11}K_2 & g_{13}-h_{11}K_3\\ g_{21}-h_{21}K_1 & g_{22}-h_{21}K_2 & g_{23}-h_{21}K_3\\ g_{31}-h_{31}K_1 & g_{32}-h_{31}K_2 & g_{33}-h_{31}K_3\end{bmatrix}$$

$$H_c=\begin{bmatrix} h_{11}K_4 & h_{12}-h_{11}K_5\\ h_{21}K_4 & h_{22}-h_{21}K_5\\ h_{31}K_4 & h_{32}-h_{31}K_5\end{bmatrix}.$$

4. Analysis of Stability and Dynamic Performance of PWM-SRC Employing Control Laws

The evaluation of the stability and dynamic characteristics for the controlled PWM-SRC with the discontinuous conduction mode is carried out using the eigenvalues of the system matrix G_c in the complex Z-plane.

The parameters used in root locus plots and dynamic simulations are given as follows :

Table 1 Coefficients of (20) for the linearized control laws of PWM-SRC

Control \ Coefficient	K1	K2	K3	K4	K5
ASDTIC Control	$\frac{g_{31}}{h_{31}}$	$\frac{g_{32}}{h_{31}}$	$\frac{g_{33}-1}{h_{31}}+\frac{Z\cdot\gamma\cdot NC}{R_L\cdot h_{31}}$	$\frac{NC\cdot Z\cdot\gamma}{h_{31}}$	$\frac{h_{32}}{h_{31}}$
Inductor-current control	$\frac{g_{11}}{h_{11}}$	$\frac{g_{12}}{h_{11}}$	$\frac{g_{13}}{h_{11}}$	$\frac{1}{h_{11}}$	$\frac{h_{12}}{h_{11}}$
Capacitor-voltage control	$\frac{g_{21}}{h_{21}}$	$\frac{g_{22}}{h_{21}}$	$\frac{g_{23}}{h_{21}}$	$\frac{1}{h_{21}}$	$\frac{h_{22}}{h_{21}}$
Optimal-trajectory control	$\frac{OP1\cdot g_{11}+g_{21}}{OP2}$	$\frac{OP1\cdot g_{12}+g_{22}}{OP2}$	$\frac{OP1\cdot g_{13}+g_{23}}{OP2}$	$\frac{OP1+1}{OP2}$	$\frac{OP1\cdot h_{12}+h_{22}}{OP2}$
	Where $OP1=\frac{Z^2\cdot x_1}{(x_2+x_3)}$, $OP2=OP1\cdot h_{11}+h_{21}$				

$$V_i = 100\,V,\ L = 0.113mH,\ C = 0.12\mu H,\ C_o = 50\,\mu F \tag{22}$$

For the convenient use of the results, the normalized output current(NOC) and the normalized output voltage(NOV) are employed as

$$NOC = (v_o \cdot Z)/(R_L \cdot v_i),\quad NOV = v_o/v_i\ . \tag{23}$$

The eigenvalues are obtained by decreasing the NOC(increasing the load R_L) for a given NOV.

Fig. 5 shows the root locus of the PWM-SRC with the transistor conduction angle control.

The eigenvalue r_3 approaching to the unit circleis dominated by the slow output filter. But, according to NOC, there is a wide variation of the eigenvalue r_2 for the given NOV. As can be seen in Fig. 5(b), when NOC is between 0.5519 and 0.3452, the oscillatory transient response will be appeared in the resonant tank and output voltage. Decreasing NOC less than 0.3452, the system has the eigenvalues on the real axis of the Z-plane which result in an overdamped transient response. It is noted from Fig. 6 and 7 that the PWM-SRC employing the ASDTIC control and the inductor-current control has the stability problem. Therefore, the stable regions of these control laws are examined and shown in Fig. 10 and 11. The root locus for the capacitor-voltage controlled PWM-SRC is shown in Fig. 8. The range of the eigenvalue r_2 in the PWM-SRC with the capacitor-volta-ge control is narrower than that of the transistor-conduction angle control. It can be said

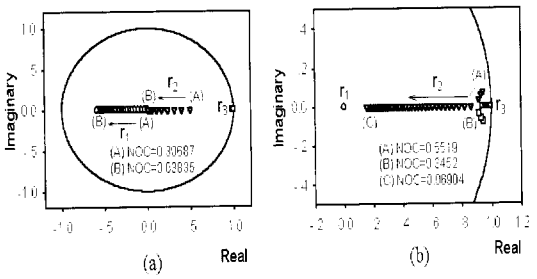

Fig. 5 Root locusfor the transistor-conduction angle controlled PWM-SRC
(a) NOV = 0.5 (b) NOV = 0.9

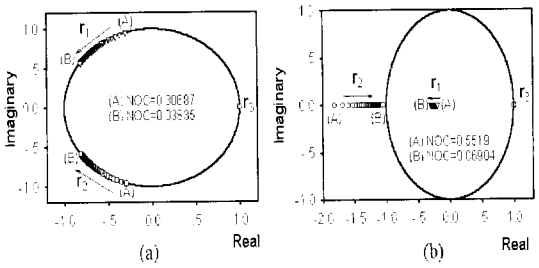

Fig. 6 Root locus for the ASDTIC controlled PWM-SRC (a) NOV = 0.5 (b) NOV = 0.9

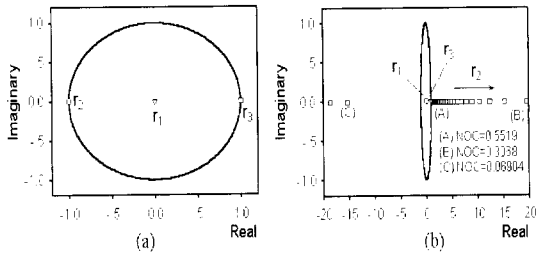

Fig. 7 Root locus for the inductor-current controlled PWM-SRC
(a) NOV = 0.5 (b) NOV = 0.9

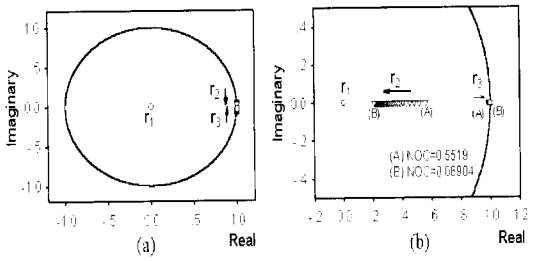

Fig. 8 Root locus for the capacitor-voltage controlled PWM-SRC
(a) NOV = 0.5 (b) NOV = 0.9

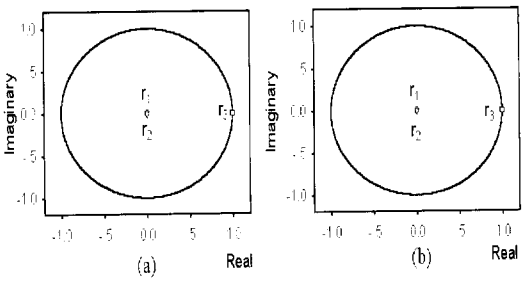

Fig. 9 Root locus for the optimal-trajectory controlled PWM-SRC
(a) NOV = 0.5 (b) NOV = 0.9

that the capacitor-voltage controlled PWM-SRC is not sensitive to the load variation than the transistor-conduction angle controlled PWM-SRC. However, the dynamic performance of this control is greatly dependent on whether NOV is low or high and this can be improved considerably at higher NOV.

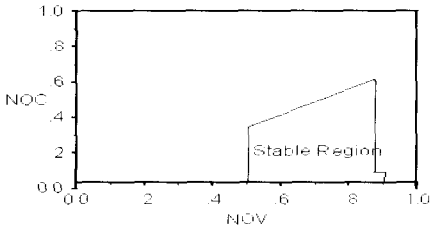

Fig. 10 Stable region for ASDTIC control

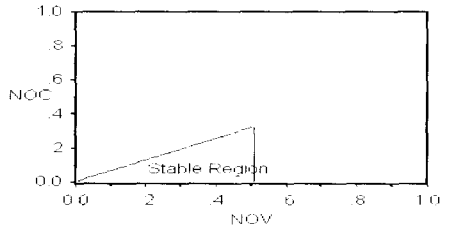

Fig. 11 Stable region for inductor-current control

Fig. 9 shows the root locus for the optimal trajectory controlled PWM-SRC. In this control method, the two eigenvalues dominated by the resonant tank are always close to the origin of the Z-plane. It indicates that the resonant tank of the PWM-SRC employing this control law always has the fastest dynamics without overshoot. For the PWM-SRC with the available control methods which are the transistor-conduction angle control, capacitor-voltage control, and optimal-trajectory control, the transient responses of the output voltage and the inductor current of the resonant tank are examined and compared to a step load variation of NOC between 0.2263($R_L = 122\Omega$) and 0.4383 ($R_L = 63\Omega$) for a given NOV of 0.9.

These are shown in Fig. 12 through 14. At the instant of the load change, the new control input is obtained by the control law to maintain the desired output voltage. Fig. 12 shows that the transient response of the PWM-SRC employing the transistor-conduction angle control is oscillatory for NOC of 0.4383 and overdamped for NOC of 0.2263. This is already predicted from the root locus shown in Fig. 5(b). The transient response of the capacitor-voltage controlled PWM-SRC shown in Fig. 13 is overdamped for the same load change, which indicates that this control is robuster to the load change than the transistor-conduction angle control.

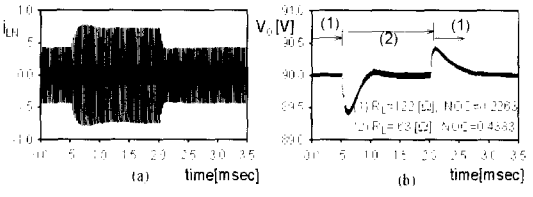

Fig. 12 Response of transistor-conduction angle control for step load change when NOV = 0.9
(a) inductor current (b) output voltage

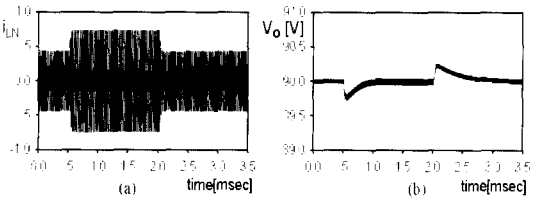

Fig. 13 Response of capacitor-voltage control for step load change when NOV = 0.9
(a) inductor current (b) output voltage

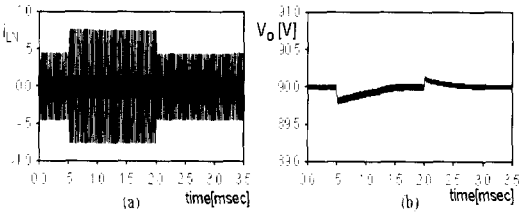

Fig. 14 Response of optimal-trajectory control for step load change when NOV=0.9
(a) inductor current (b) output voltage

As shown in Fig. 14(a), the inductor current of the PWM-SRC with the optimal-trajectory control has the fastest transient response. It

can be noted that the order of the optimal-trajectory controlled PWM-SRC is reduced by two. But, in this control, the transient response of the output voltage is slow. This can be explained from the fact that the eigenvalue r_3 dominated by the output filter is close to the unit circle. However, it can be improved by adding the output voltage feedback loop.

5. Conclusion

In this paper, employing the linearized small signal model, several different control methods are identified and their stability and dynamic responses are evaluated. The PWM-SRC with the transistor-conduction angle control is found to be stable from this evaluation. It is, however, sensitive to the load variation than that with capacitor-voltage control. When the PWM-SRC employs the ASDTIC control or the inductor-current control, there exists stability problem. Thus, the stable regions of these control laws are investigated and illustrated. The capacitor-voltage controlled PWM-SRC has a good dynamic response for the higher NOV and the system with this control is relatively robust for the load variation. However, the dynamic performance of this control is greatly dependent on whether NOV is low or high. For the PWM-SRC in discontinuous conduction mode, the optimal-trajectory control method is proposed and designed so that the two dominant eigenvalues characterized by the resonant tank can be located closely to the origin of the complex Z-plane in a time-optimal manner. Therefore, using this control method, the stability and dynamic characteristics of the PWM-SRC can be remarkably improved and these are confirmed by simulation results.

참 고 문 헌

[1] V. Vorperian, "Approximated Small Signal Analysis of the Series Resonant Converters", IEEE Trans. Power Electron., vol. 4, no. 4, pp. 15-24, 1989.

[2] M. E. Elbuluk, and G. C. Verghese, Sampled-data modeling and digital control of resonant converters, IEEE Trans. On Power Electronics, vol. 3, no. 3, pp. 344 354, 1988.

[3] R. Oruganti, and F. C. Lee, Resonant power processor. Part II Methods of Control, IEEE Trans. on Industry Applications, vol. 21, no. 6, pp. 1461-1471, 1985.

[4] Jean-pierre Vandelac, and Phoivos D. Ziogas, A DC to DC pwm series resonant converter operated at resonant frequency, IEEE Trans. on Industrial Electronics, vol. 35, no. 3, pp. 451 460, 1988.

[5] Juan A. Sabate, and F. C. Lee, Off line application of the fixed frequency clamped mode series resonant converter, IEEE Trans. on Power Electronics, vol. 6, no. 1, pp. 39 47, 1991.

[6] H. C. Choi, G. W. Moon, and M. J. Youn, Small signal modelling for the PWM series resonant converter, International Journal of Electronics, vol. 75, no. 5, pp. 985-997, 1993.

저 자 소 개

최현칠(崔鉉七)

1964년 5월 25일생. 1989년 경희대 공대 전자공학과 졸업. 1991년 한국과학기술원 전기 및 전자공학과 졸업(석사). 1994년 동대학원 졸업(공박). 1994~1995년 한국과학기술원 정보전자연구소 연구원. 1995년~1996년 대우전자 모니터 연구소 선임연구원. 1997년~현재 인제대 전자정보통신공학부 조교수.